

# Prediction of Tire/Wet Road Friction and its Variation with Speed from Road Macro- and Microtexture, and Tire-Related Properties

**Minh-Tan Do**

Civil Engineer, Corresponding Author, LCPC, Route de Bouaye, BP 4129, 44341 Bouguenais, France, [minh-tan.do@lcpc.fr](mailto:minh-tan.do@lcpc.fr).

**Yves Delanne**

Research Director, LCPC, Route de Bouaye, BP 4129, 44341 Bouguenais, France, [yves.delanne@lcpc.fr](mailto:yves.delanne@lcpc.fr).

## ABSTRACT

In this paper, validation of a model for the speed dependency of friction is presented. Based on the shape of the friction – speed curve, the model assumes that calculation of friction at any speed would need an estimate of friction at very low speed, and the knowledge of its variation with speed described by the Stribeck curve.

Two existing models developed at LCPC are then coupled to predict friction versus speed from the following characteristics: road surface macro and microtexture, rubber relaxation time, wheel slip, tire tread depth and water layer thickness. Description of the models is given.

The unified model is validated on data obtained from experimental campaigns conducted in France from 2001 to 2003. On 30 sections, including test tracks and trafficked roads, friction was measured by means of the British Pendulum and the front-wheel braking method with the LCPC instrumented car giving  $\mu_{\text{peak}}$  and  $\mu_{\text{locked}}$ . Road-microtexture profiles were measured by means of LCPC static laser systems. Profile characteristics are given.

BPN and  $\mu_{\text{peak}}$  values were compared with results predicted from road microtexture and tire-rubber properties. For  $\mu_{\text{locked}}$ , which is obtained at higher speeds, its value was deduced from  $\mu_{\text{peak}}$  using the modelled Stribeck curve. Results are discussed.

# Prediction of Tire/Wet Road Friction and its Variation with Speed from Road Macro- and Microtexture, and Tire-Related Properties

## INTRODUCTION

The friction between a tire and a wet road surface varies with the vehicle speed, due to the mutual influence of water and road surface texture. The knowledge of the speed dependency of friction is important for various applications: estimation of the braking distance, assessment of the pavement skid-resistance, etc.

In [1], it is shown that the friction – speed curve has a general inverse-S shape (Fig. 1). From literature review [2][3], it is found that this shape is typical for lubricated contact and is known as the “Stribeck curve”. From the figure 1, it can be seen that the calculation of wet friction coefficients for a tire/road couple at any speed would need: an estimate of the friction coefficient at very low speed ( $\mu_{ls}$ ) (say lower than 20km/h) and the knowledge of the Stribeck curve describing the decrease of  $\mu_{ls}$  with speed.

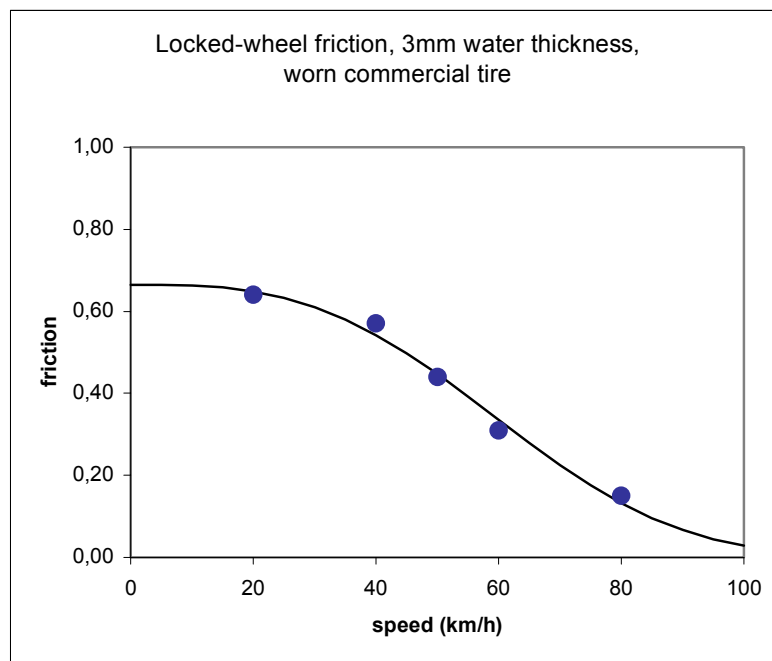


**Figure 1. General shape of friction – speed curve**  
(Data source: CETE Lyon)

At LCPC, research has been started in the nineties to better understand the influence of road surface microtexture on friction. Relevant microtexture descriptors are defined and a contact model called “Stefani model” is developed to calculate very-low-speed friction from these descriptors [4]. More recently, another model is developed to describe the Stribeck curve for monitoring and commercial tires on various road surfaces [5]. It is then tempting to couple both models to estimate the friction – speed curve from road- and tire measurable parameters. The work carried out is presented in this paper.

## PREVIOUS WORKS

### Model for Stribeck curve

In [5], it is shown that typical friction – speed curves (linear, exponential) represent parts of the more general Stribeck curve. The following formula is proposed to describe the inverse-S shape [5]:

$$\mu = \mu_0 \exp\left[-\left(\frac{V}{V_s}\right)^\delta\right] + \gamma V \quad (1)$$

Where

- $\mu$ : friction;
- $\mu_0$ : friction at theoretical zero speed;
- $V_s$ : so-called “Stribeck” speed;
- $\delta$ : constant defining the curve shape;
- $\gamma$ : constant defining the “viscous” component of friction.

The model represented by (1) is called the “modified exponential model”. It can be seen that the well-known PIARC model [6] is a particular case of the formula (1) ( $\delta = 1$  and  $\gamma = 0$ ).

In [5], it is shown that  $\mu_0$  is strongly related to the British Pendulum Number (BPN). It could be explained by the fact that, according to the shape of the full line in the figure 1, friction is almost constant in the low-speed region and consequently, friction at theoretical zero speed is in the same order as friction at speed lower than say 20km/h, in particular BPN (measured at roughly 10km/h). So it can be said that  $\mu_0 = \mu_{ls}$ .

The constant  $V_s$ , which is very similar in the spirit to the “speed constant” of the PIARC model, is shown to depend on the surface macrotexture and the wheel slip [5]. Analysis of a significant data base acquired within the frame of the FEHRL HERMES (Harmonization of European Routine and Research Measuring Equipment for Skid Resistance of Roads and Runways) project gives the following formula:

$$V_s = 117MPD^a \kappa^{0.9} \quad (2)$$

Where

- MPD: Mean Profile Depth as defined by ISO standard 13473 [7];
- $\kappa$ : wheel slip;
- a: device-dependent constant.

The wheel slip (braking) is defined by the following formula:

$$\kappa = \frac{V - R\omega}{V}$$

Where

- V: longitudinal speed;
- R: tire radius;
- $\omega$ : angular velocity of the tire.

The constant  $\delta$ , which controls the friction – speed curve shape, is found to vary with the water layer thickness and the tire tread depth [5]. In the figure 2, except some abnormal values (circled points), the variation of  $\delta$  with the ratio

water thickness/tire tread depth (WD/TD) shows a rapid increase of  $\delta$  then a stabilization when  $WD/TD > 1$ . The threshold  $WD/TD = 1$  for a given tire gives the critical water thickness which saturates completely the tire pattern grooves.

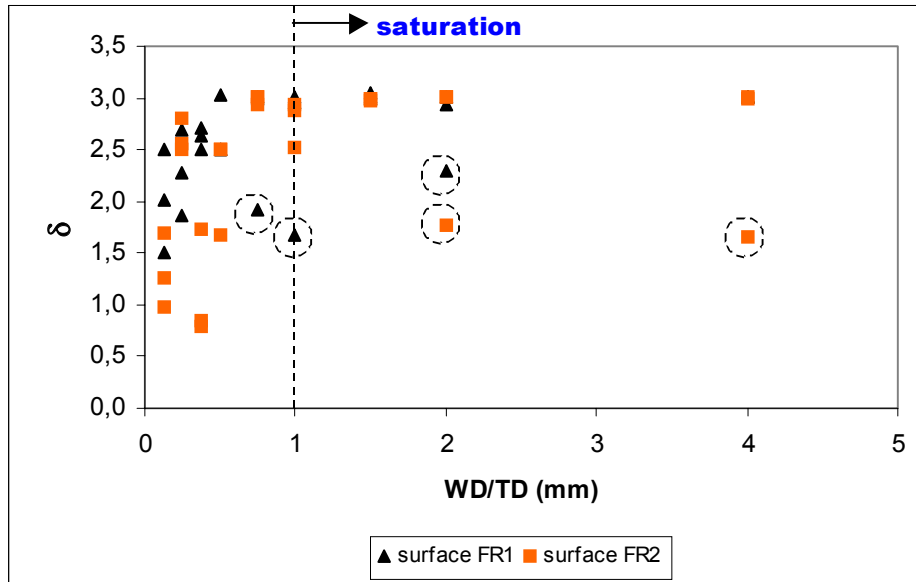


**Figure 2. Variation of  $\delta$  with  $WD/TD$**   
(*WD: water depth, TD: tire tread depth*)

The last remark is that  $\gamma$  is negligible. Analysis of data from VERT (**VE**hicle **R**oad **T**ire Interaction) project related to one tire [5] shows that, except a few cases,  $\gamma$  value is always less than  $10^{-4}$ , meaning that the corresponding friction is not more than 0.01 (the maximum test speed is 90km/h).

### Microtexture descriptors

The microtexture descriptors are detailed in [4]; they are briefly reminded here.

Example of road profiles is shown in the figure 3. The Y-scale shows that the observed scale is the surface microtexture. The characterization method is based on the following established facts:

- Friction is generated only in direct-contact spots between the tire and the road surface;
- The road-asperity shape is the most relevant factor for friction generation.

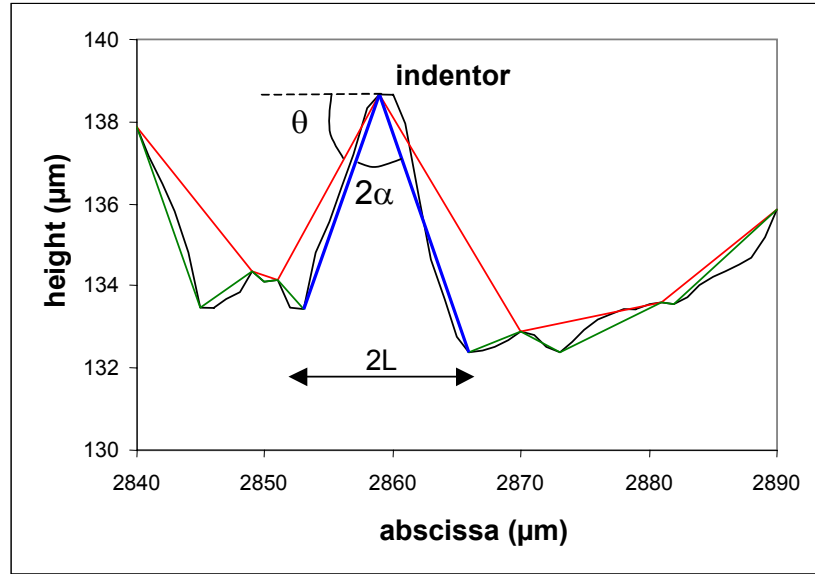


**Figure 3. Road profile and microtexture descriptors**

Road asperities where contact occurs are defined as “indentors” (Fig. 3). An indenter is then part of the profile between two valleys. The indenter distribution is characterized by two parameters: the shape (cotangent of angle  $\alpha$ ) and the relief (angle  $\theta$ ). Simple algorithm is developed to detect all profile peaks and valleys called “extremes”.

The characteristic angles are calculated by means of the following formulae:

$$\alpha = \frac{1}{2} \times \left[ \tan^{-1} \left| \frac{x_i - x_{i-1}}{z_i - z_{i-1}} \right| + \tan^{-1} \left| \frac{x_{i+1} - x_i}{z_{i+1} - z_i} \right| \right] \quad (3)$$

Where

$x_i$ : abscissa of the  $i^{\text{th}}$  extreme (if index (i) is a peak, the indexes (i-1) and (i+1) are valleys);  
 $z_i$ : height of the  $i^{\text{th}}$  extreme.

And

$$\theta = \tan^{-1} \left| \frac{z_{j+1} - z_j}{x_{j+1} - x_j} \right| \quad (4)$$

Where

$x_j$ : abscissa of the  $j^{\text{th}}$  peak;  
 $z_j$ : height of the  $j^{\text{th}}$  peak.

### Stefani contact model

This contact model is developed by M. Stefani (LCPC researcher) with the original aim to simulate the hysteresis effect of friction (energy loss by viscoelastic properties of the rubber). The model geometry represents the contact between a rubber pad and part of a road profile between two peaks called “motif” (Fig. 4). No surface friction (adhesion) is considered. Therefore, the model assumes that friction forces are generated uniquely by deformation

of the Kelvin solid representing the rubber pad. The relaxation time of this solid (ratio  $\eta/K$ ) is used as the rubber characteristic. It should be noted that the Stefani model is developed for microtexture-study purpose, so the calculated friction is low-speed.

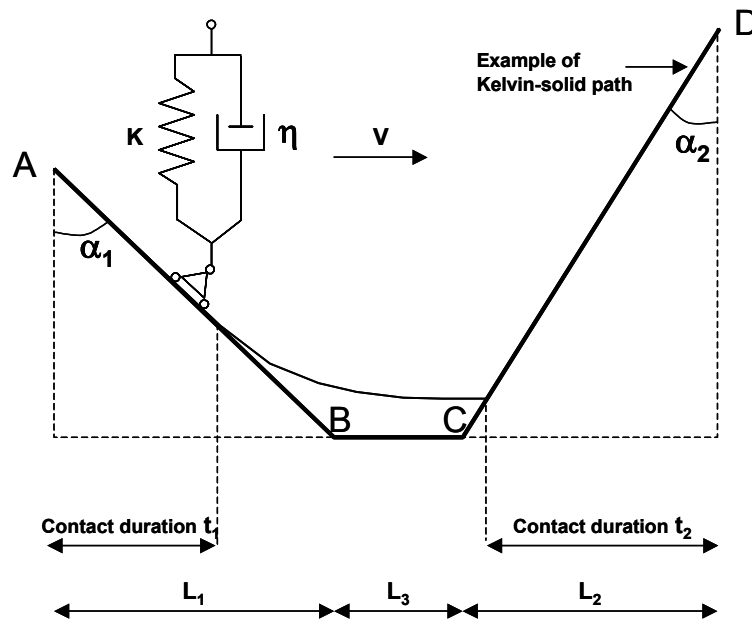


Figure 4. Geometry of the contact model

Due to the motif geometry, contact loss can occur between the solid and the motif. Vertical and horizontal forces are calculated and integrated over the contact durations  $t_1$  and  $t_2$ . The ratio between their resultants ( $f_v$  and  $f_h$  respectively) is defined as a coefficient of friction  $\mu$ . Details of the calculations can be found in [4].

By setting  $L_3 = 0$ , this contact model can be coupled with the characterization method developed above to calculate  $\mu$  from road profiles. The first results [4] obtained on laboratory surfaces composed of coarse aggregates show that two friction values must be considered, which correspond to  $\mu$  calculated at two scales: the “roughness” scale related to the profile and the “undulation” scale related to its envelop (line connecting all profile peaks). Indentors of the roughness scale are determined from the “green” line of the figure 3, and those of the undulation scale from the “red” line (Fig. 3).

## VALIDATION ON ACTUAL ROAD SURFACES

### Experimental program

Within the frame of a 4-year LCPC project, seven road-test campaigns were carried out from 2001 to 2003. The main objective is to gather on the same road surface all texture- and friction information. Each campaign includes the following tasks:

- Friction measurements: deceleration tests, BPN tests [8];
- Texture measurements: macrotexture (volumetric method [9]) and microtexture (road profiles);
- Core sampling, when it was possible.

The volumetric tests were performed using glass beads. The test results are the standardized Mean Texture Depth (MTD) [7]. The test sites included trafficked roads and test tracks. Their selection was based on the consideration of the mix formulation, the aggregates and the skid-resistance.

Deceleration tests and macrotexture measurements were done on road. BPN tests and microtexture-profile measurements were done on road surfaces when there was no core sampling, or in laboratory on specimens when core sampling was possible. Scheme of a typical test section with respective locations for BPN tests, volumetric and road profile measurements, and core sampling is illustrated in the figure 5.

Microtexture profiles were sampled every 10µm. On road, since time is limited, only one profile of 200mm long is measured. In laboratory, 13 profiles of 80mm long were measured on each specimen.

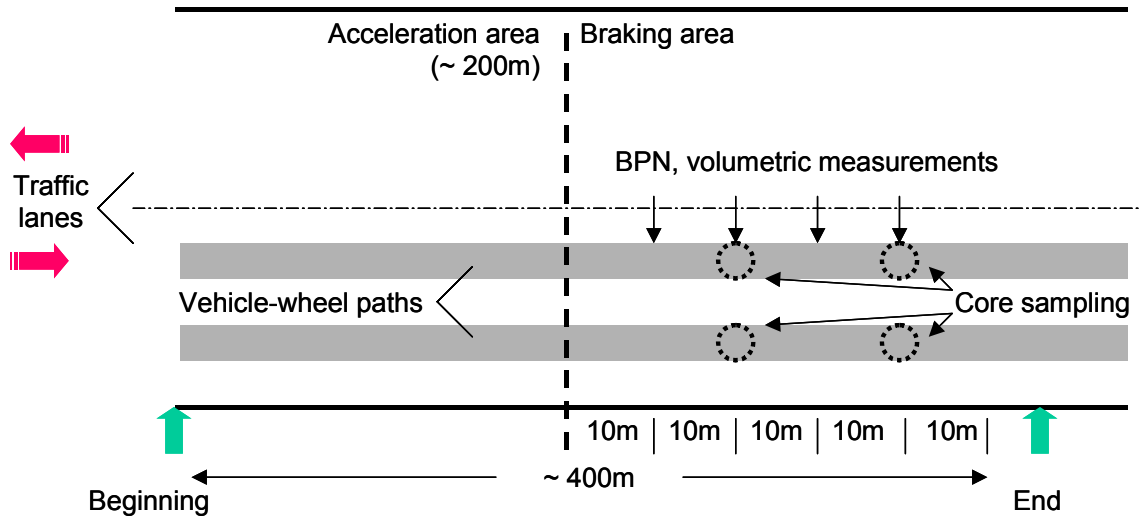


Figure 5. Typical test section

### Deceleration tests and friction estimation

Front-wheel braking tests are performed by means of a light instrumented vehicle (Peugeot 406) with and without ABS activation (Fig. 6). Surfaces are wetted by a tank truck. Decelerations are recorded between two speeds  $V_1$  and  $V_2$ , then the brake is released. Tests are performed for two ranges of speeds: 90km/h ( $V_1$ ) to 70km/h ( $V_2$ ), and 60km/h ( $V_1$ ) to 40km/h ( $V_2$ ).



**Figure 6. LCPC instrumented vehicle**

Friction is estimated from the average deceleration by the following formula:

$$\mu = \frac{M \left[ \left[ \frac{V_1^2 - V_2^2}{2 \cdot d} \right] - \left[ A + B \cdot \left( \frac{V_1 + V_2}{2} \right)^2 \right] \right]}{Z_{av} + M \cdot \left( \frac{V_1^2 - V_2^2}{2 \cdot d} \right) \cdot \frac{h}{L}} \quad (5)$$

Where

- $\mu$ : estimated friction;
- M: vehicle mass;
- d: braking distance;
- $V_i$  (i = 1, 2): test speed;
- $Z_{av}$ : load on the front axle;
- h: height of the vehicle center of gravity (Fig. 6);
- L: vehicle wheelbase (Fig. 6).

A, B: rolling-resistance coefficients (rolling-resistance force =  $M \cdot \left[ A + B \cdot \left( \frac{V_1 + V_2}{2} \right)^2 \right]$ ).

The estimation is  $\mu_{peak}$  (respectively  $\mu_{locked}$ ) for braking with ABS (respectively without ABS). The associated speeds are the mean of the speed range: 80km/h for high-speed deceleration test and 50km/h for low-speed deceleration test. For the estimated  $\mu_{peak}$ , the related tire slip-speed (product speed  $\times$  wheel slip) is low since the wheel slip  $\kappa$  corresponding to the ABS activation is roughly 0.1.

## Results

Based on the modified exponential model and the Stefani model, the complete friction – speed curve can be estimated by the following way:

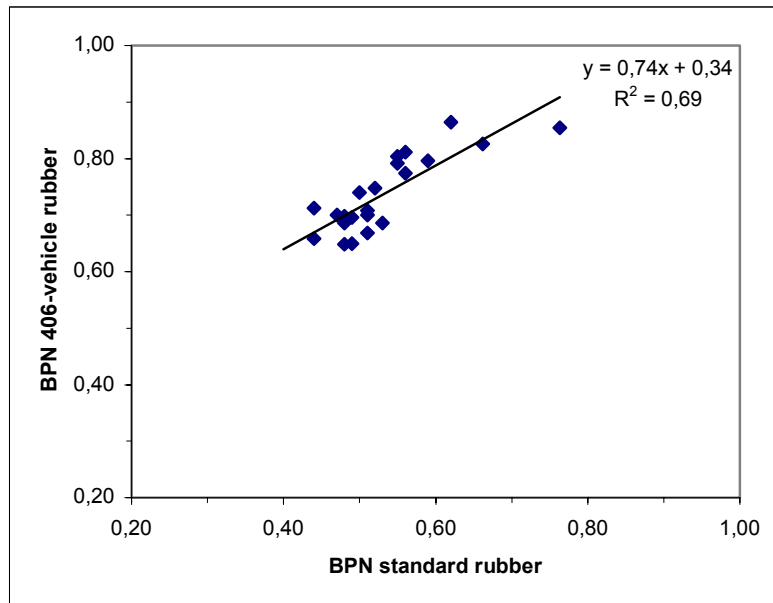
- Estimation of  $\mu_0$  from road-surface microtexture using the Stefani model;
- Estimation of  $V_s$  from road-surface macrotexture and wheel slip (formula (2));
- Estimation of the decrease of  $\mu_0$  with speed using the modified exponential model (formula (1)).

The following points are checked:

- The prediction of BPN and  $\mu_{peak}$  from road surface microtexture by the Stefani model;
- The correspondence between BPN and  $\mu_{peak}$ . Can we consider  $\mu_{ls} = \mu_0 \approx BPN \approx \mu_{peak}$  ?
- The prediction of  $\mu_{locked}$  from the knowledge of  $\mu_0$  and the Stribeck curve.

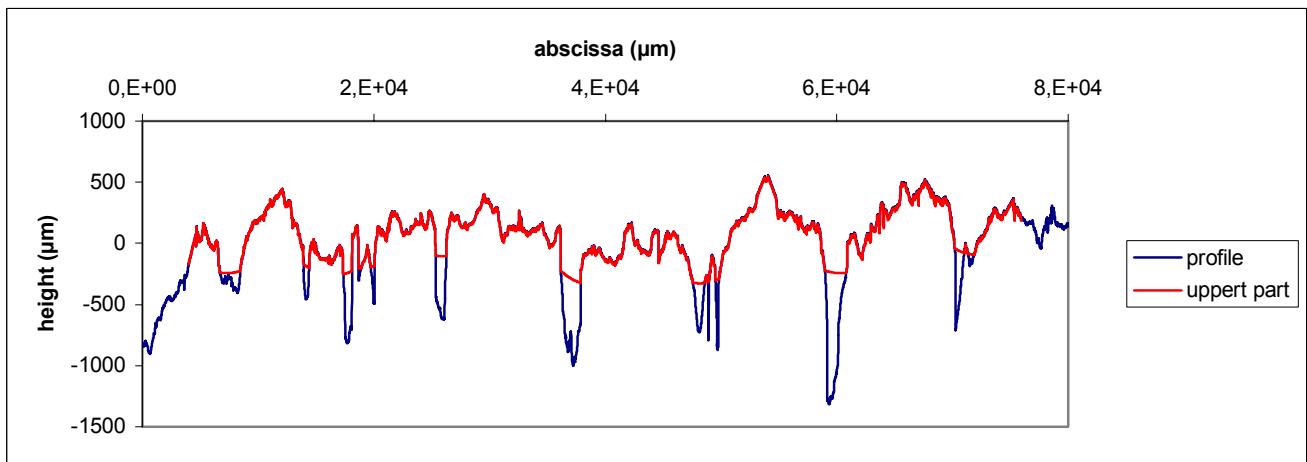
Since it is well known that rubber properties affect friction, preliminary comparison is made between BPN measured with two rubber pads: one made from the standard rubber [8] and one from the tire rubber (front wheels) of the instrumented vehicle. Results are shown in the figure 7. It can be seen that BPN values depend on the employed rubber. It is then decided to use the values obtained with the tire rubber for further comparisons.





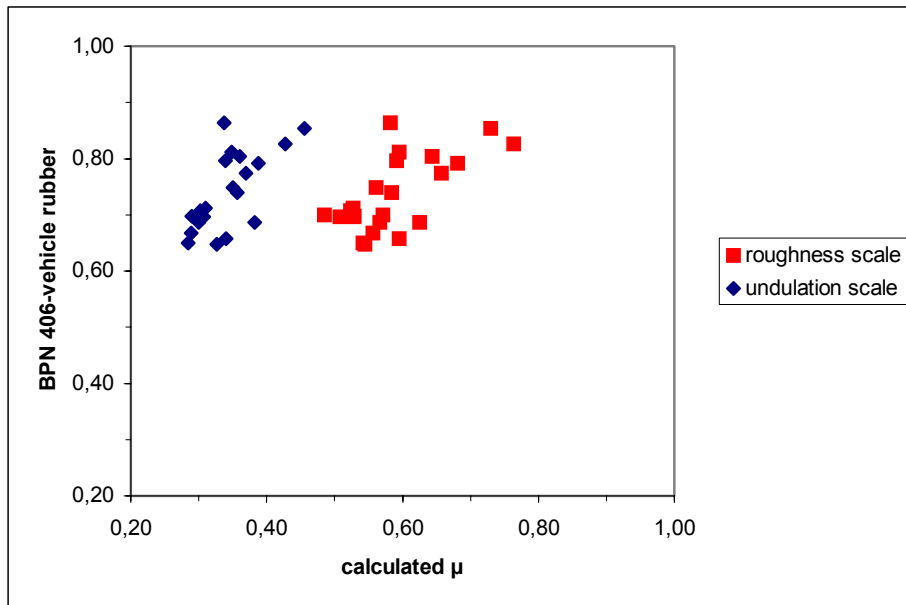
**Figure 7. Influence of rubber on BPN**

Regarding the profile analysis, preliminary investigations show that the analysis must be limited to the upper part of the profiles, say roughly 0.5 to 1mm. This statement is supported by the fact that the correlation between microtexture descriptors and BPN is better for filtered profiles compared with unfiltered profiles (unpublished results). A mathematical tool is developed to extract this part from the whole profile. Example is shown in the figure 8.



**Figure 8. Example of profile filtering**

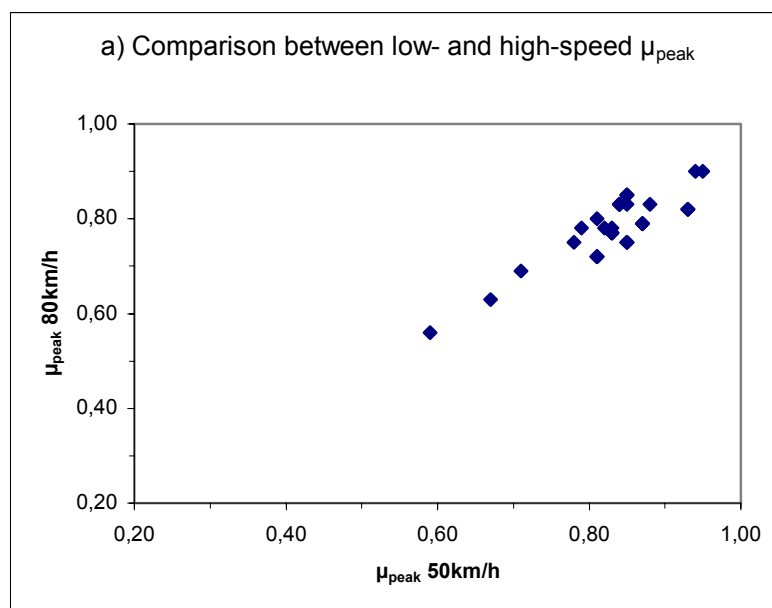
Comparison between measured surface-BPN and calculated friction at the roughness- and undulation scale is shown in the figure 9. Despite some scatter, fair tendency is found. Friction at the roughness scale is closer to BPN than friction at the undulation scale. It does mean that all profile indentors contribute to friction in BPN test and therefore must be taken into account for in the model.



**Figure 9. Comparison between BPN and  $\mu$  calculated from Stefani model**

Regarding  $\mu_{\text{peak}}$ , a first comparison is made between  $\mu_{\text{peak}}$  at 80km/h (sliding speed  $\approx 8$  km/h) and 50km/h (sliding speed  $\approx 5$ km/h). It can be seen from the figure 10a that in a first step their differences can be neglected. Further comparison between  $\mu_{\text{peak}}$  and BPN shows significant scatter, even if the “cloud” is close to the graph bisector (Fig. 10b). The scatter can be due to the number of BPN-test zones, which are not representative enough compared with the braking distance.

Despite some scatter due to sampling problem, results from the figure 10 show that BPN and  $\mu_{\text{peak}}$  at 50km/h and 80km/h are comparable. Since the slip speeds associated to these friction values are low ( $< 15$ km/h), these results are going to confirm the existence of the stable-friction zone of the Stribeck curve in low-speed region (Fig. 1).



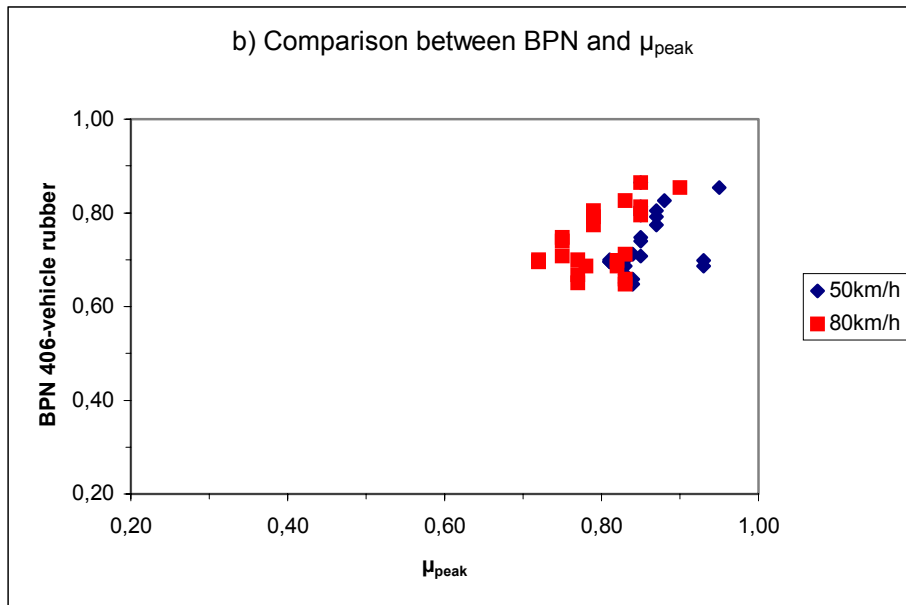
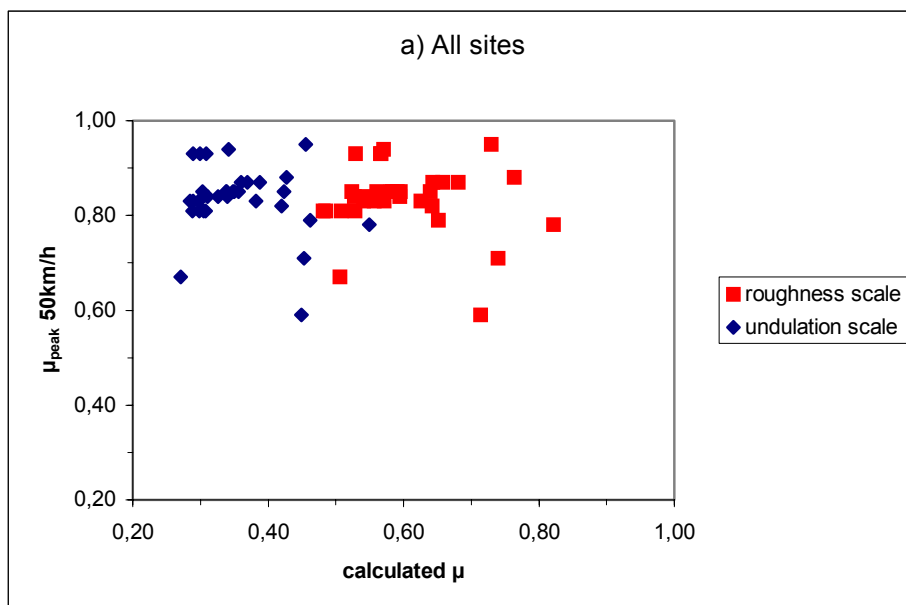
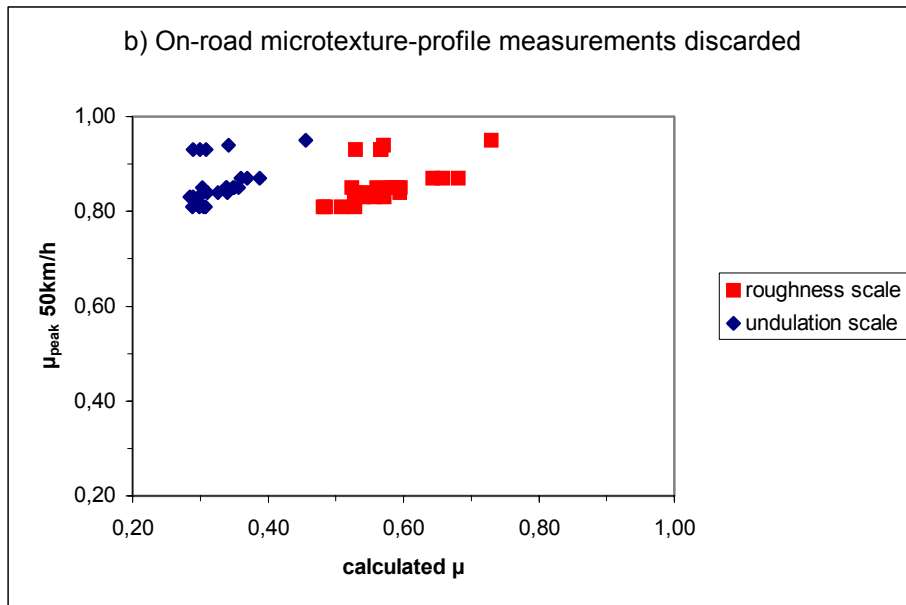


Figure 10. Comparison between BPN, low- and high-speed  $\mu_{\text{peak}}$

Comparison between  $\mu_{\text{peak}}$  at 50km/h and calculated friction is shown in the figure 11. Big scatter can be seen (Fig. 11a). Closer examination of individual results displays two groups corresponding to microtexture-profile measurements on road and in laboratory respectively. It is found that scatter is due to measurements on road. Since no artifact is found, assumption is made on the insufficient microtexture-profile sampling on roads, but it needs to be investigated. Suppression of on-road points gives a fairer tendency (Fig. 11b).



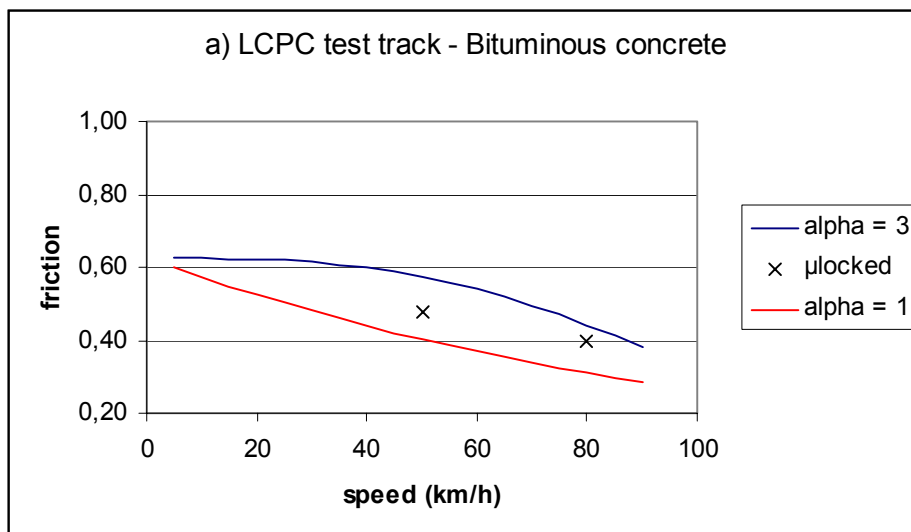


**Figure 11. Comparison between  $\mu_{\text{peak}}$  and  $\mu$  calculated from Stefani model**

For the prediction of  $\mu_{\text{locked}}$ , the following procedure is adopted:

- Calculation of two Stribeck curves for two extreme values of  $\alpha$  derived from the figure 2 ( $1 < \alpha < 3$ ). They constitute the extremes friction – speed curves;
- On the friction – speed graph, comparison between measured values ( $\mu_{\text{locked}}$  at 50km/h and 80km/h) and theoretical curves.

Examples of validation results are shown the figure 12. From both graphs, it can be seen that the comparison is satisfactory despite some approximations (calculation of  $V_s$  from MTD instead of MPD, uncertainty in the estimation of  $\mu_0$ ), since the experimental points are whether close to theoretical curve (Fig. 12b) or inside the zone delimited by the extremes (Fig. 12a).



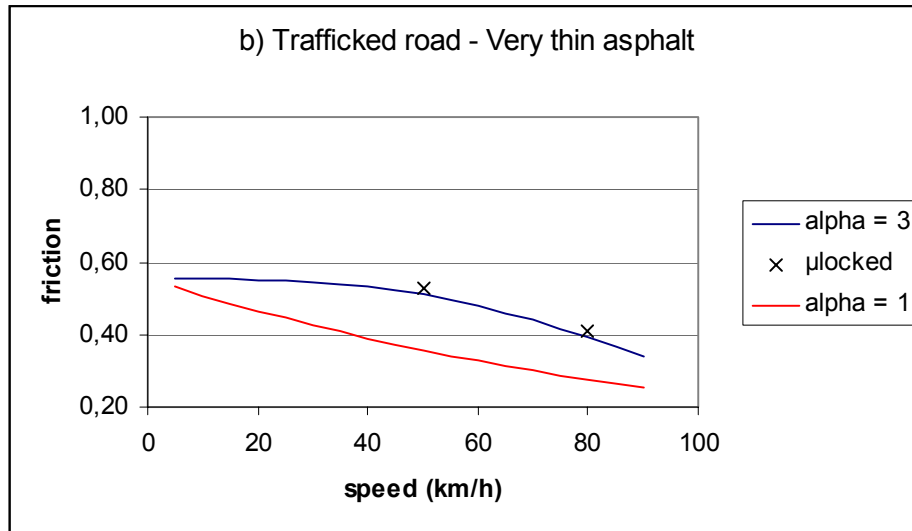


Figure 12. Comparison between  $\mu_{\text{locked}}$  and Stribeck curves

## CONCLUSIONS

In this paper, validation of a model for the speed dependency of friction is presented. Based on the shape of the friction – speed curve, the model assumes that the calculation of friction at any speed would need an estimate of friction at very low speed, and the knowledge of its variation with speed described by the Stribeck curve.

Two existing models developed at LCPC are then coupled to predict friction versus speed from the following characteristics: road surface macro- and microtexture, rubber relaxation time, wheel slip, tire tread depth and water layer thickness. Description of the models is given.

The unified model is validated on data obtained from road tests conducted in France from 2001 to 2003. Despite some scatters, the following conclusions can be settled:

- BPN and  $\mu_{\text{peak}}$  values are highly related and can be estimated from road-surface microtexture and tire rubber relaxation time;
- The Stribeck curve can be a base from which it is possible to predict  $\mu_{\text{locked}}$  from the knowledge of friction estimated from the Stefani model and its variation with speed.

The great scatter observed in some comparisons show that many efforts are still needed before the prediction of friction from surface microtexture is solved. The following problems are raised from this work:

- Profile measurement. The profile fineness (10 $\mu\text{m}$ ) seems to be sufficient. However, a sampling procedure needs to be investigated to provide representative profiles regarding the friction process.
- Profile analysis. The analysis is done on the upper part of the profile. Mathematical tool is developed to extract mathematically this part. However, the method needs to be improved and supported by physical proofs.
- Microtexture description. The shape and relief descriptors seem to be relevant. However, robustness of the characterization needs to be improved.

New investigations are also necessary to see whether more relevant parameters than MPD regarding macrotexture are to be introduced in the friction – speed curve.

## REFERENCES

- [1] F. La Torre, L. Domenichini, "*Friction Prediction Models*", Proceedings of the 2<sup>nd</sup> International Colloquium on Vehicle Tire Road Interaction, 23<sup>rd</sup> Feb. 2001, paper 01.08B, pp. 133-147, 2001.
- [2] M.M.J. Jacobs, W. Gerritsen, M.P. Wennink, F. van Gorkum, "*Optimisation of Skid Resistance Characteristics with Respect to Surface Materials and Road Function*", Proceedings of the 3<sup>rd</sup> International Symposium on Pavement Surface Characteristics, 3-4 Sept 1996, Christchurch, New Zealand, pp. 283-298, 1996.
- [3] W.C. Emmens, "*The Influence of Surface Roughness on Friction*", Proceedings of the 15<sup>th</sup> International Deep Drawing Research Group (IDDRG) Biennial Congress, Deadborn, pp. 63-70.
- [4] M.-T. Do, H. Zahouani, "*Frottement Pneumatique/Chaussée – Influence de la Microtexture des Surfaces de Chaussée*", Actes des Journées Internationales de Tribologie, 2-4 Mai 2001, Obernai, France, pp. 49-61, 2001.
- [5] M.-T. Do, P. Marsac, A. Mosset, "*Tribology Approach to Predict the Variation of Tire/Wet Road Friction with Slip Speed*", Paper submitted to 5<sup>th</sup> International Symposium on Pavement Surface Characteristics, 6-9 June 2004, Toronto, Canada.
- [6] J.C. Wambold, C.E. Antle, J.J. Henry, Z. Rado, G. Descornet, U. Sandberg, M. Gothie and S. Huschek, "*International PIARC Experiment to Compare and Harmonize Skid Resistance and Texture Measurements*", PIARC Publication n°01.04.T, Paris, 1995.
- [7] ISO 13473-1, "*Characterization of pavement texture by use of surface profiles - Part 1: Determination of Mean Profile Depth*".
- [8] PR NF EN 13036-4, « *Caractéristiques de Surface des Routes et Aéroports. Méthodes d'Essais. Partie 4 : Méthode d'Essai pour Mesurer l'Adhérence d'une Surface : l'Essai au Pendule* », Projet de norme européenne.
- [9] NF EN 13036-1, « *Caractéristiques de Surface des Routes et Aéroports. Méthodes d'Essais. Partie 1 : Mesurage de la Profondeur de Macrotecture de la Surface d'un Revêtement à l'Aide d'une Technique Volumétrique à la Tâche* », 2002.